

NEW LOW-MASS STARS AND BROWN DWARFS WITH DISKS IN THE CHAMAELEON I STAR-FORMING REGION¹

K. L. LUHMAN² & A. A. MUENCH³

Draft version November 2, 2018

ABSTRACT

We have used images obtained with the Infrared Array Camera and the Multiband Imaging Photometer onboard the *Spitzer Space Telescope* to search for low-mass stars and brown dwarfs with circumstellar disks in the Chamaeleon I star-forming region. Through optical spectroscopy of sources with red colors in these data, we have identified seven new disk-bearing members of the cluster. Three of these objects are probably brown dwarfs according to their spectral types (M8, M8.5, M8-L0). Three of the other new members may have edge-on disks based on the shapes of their infrared spectral energy distributions. One of the possible edge-on systems has a steeply rising slope from 4.5 to 24 μm , indicating that it could be a class I source (star+disk+envelope) rather than a class II source (star+disk). If so, then it would be one of the least massive known class I protostars (M5.75, $M \sim 0.1 M_{\odot}$).

Subject headings: accretion disks — planetary systems: protoplanetary disks — stars: formation — stars: low-mass, brown dwarfs — stars: pre-main sequence

1. INTRODUCTION

Observations of circumstellar accretion disks around young stars provide fundamental constraints on the processes of star and planet formation. Such studies are facilitated by the identification of large, representative samples of disk-bearing members of star-forming regions. The most obvious signature of a disk around a young star is the presence of emission at infrared (IR) wavelengths in excess above that expected from a stellar photosphere. One approach to applying this diagnostic has been to obtain mid-IR photometry ($\lambda \sim 5\text{-}20 \mu\text{m}$) for known members of star-forming regions (Kenyon & Hartmann 1995). However, the resulting sample of stars is biased by the selection criteria that were originally used to discover those objects. For instance, stars that are heavily obscured by edge-on disks, protostellar envelopes, or molecular clouds are mostly absent from optically-selected samples of young stars. Alternatively, wide-field mid-IR images of star-forming regions can be used to search for stars with disks in a relatively unbiased fashion. The feasibility of such surveys has steadily improved over the past two decades with advances in IR telescopes and detectors. The *Infrared Astronomical Satellite (IRAS)* imaged most of the sky in four mid- and far-IR bands, producing the first comprehensive census of disks around young stars. However, because of its low spatial resolution, *IRAS* was capable of resolving young stellar populations only in low-density regions like Taurus (Beichman et al. 1986; Kenyon et al. 1990). The better resolution and sensitivity of the *Infrared Space Observatory (ISO)* allowed it to extend mid-IR surveys to denser clusters and lower stellar masses, including

a few brown dwarfs (Persi et al. 2000; Comerón et al. 1998, 2000; Natta & Testi 2001; Pascucci et al. 2003). Ground-based cameras equipped with large-format IR detector arrays have offered even higher spatial resolution (Lada et al. 2000; Haisch, Lada, & Lada 2001), but are restricted to the shortest IR bands where excess emission from disks is smaller ($\lambda \sim 1\text{-}4 \mu\text{m}$).

The *Spitzer Space Telescope* (Werner et al. 2004) offers the best available combination of field of view, sensitivity, spatial resolution, and wavelength coverage for identifying young stars with disks (Allen et al. 2004; Gutermuth et al. 2004; Megeath et al. 2004; Muzerolle et al. 2004). The unique capabilities of *Spitzer* have been applied to a large number of star-forming regions (Luhman et al. 2008, references therein). One of the primary objectives of these surveys is the extension of previous samples of disk-bearing stars to lower stellar masses. In an attempt to reach the lowest possible masses, *Spitzer* data have been used to search for new low-mass stars and brown dwarfs with disks in the nearest molecular clouds, including Taurus (Luhman et al. 2006), Perseus (Muench et al. 2007), Lupus (Allen et al. 2007), Chamaeleon, and Ophiuchus (Allers et al. 2006, 2007; Luhman et al. 2005, 2008). We have continued this work by performing optical spectroscopy on candidate low-mass objects in Chamaeleon I ($d = 160\text{-}170 \text{ pc}$, Whittet et al. 1997; Wichmann et al. 1998; Bertout et al. 1999). In this paper, we describe the selection of these candidates from *Spitzer* images (§ 2) and measure their optical spectral types (§ 3). We then characterize the stellar parameters, spatial distribution, and spectral energy distributions of the confirmed members (§ 4) and summarize their notable properties (§ 5). In the Appendix, we present measurements of *Spitzer* photometry for all known members of Chamaeleon I that appear in the latest images of the region.

¹ Based on observations performed with the Magellan Telescopes at Las Campanas Observatory and the *Spitzer Space Telescope*.

² Department of Astronomy and Astrophysics, The Pennsylvania State University, University Park, PA 16802; kluhman@astro.psu.edu.

³ Harvard-Smithsonian Center for Astrophysics, Cambridge, MA 02138.

2. SELECTION OF CANDIDATE MEMBERS OF CHAMAELEON I

To search for new disk-bearing members of Chamaeleon I, we use images at 3.6, 4.5, 5.8, and 8.0 μm obtained with *Spitzer's* Infrared Array Camera (IRAC; Fazio et al. 2004) and images at 24 μm obtained with the Multiband Imaging Photometer for *Spitzer* (MIPS; Rieke et al. 2004). We consider all observations of this kind that have been performed in Chamaeleon I, most of which were reduced and analyzed by Luhman et al. (2008). The photometric catalog produced by Luhman et al. (2008) is used for this study. The remaining observations of Chamaeleon I that were not examined by Luhman et al. (2008) were obtained through the *Spitzer* Legacy program of L. Allen, which has a program identification of 30574. The Astronomical Observation Request (AOR) identifications are 19986432, 19992832, 20006400, 20012800, 20014592, and 20015104 for the IRAC observations and 19978496, 19979264, 20010240, and 20011008 for the MIPS observations. The IRAC and MIPS images were collected on 2007 May 15-17 and 2007 April 5 and were processed with the *Spitzer* Science Center (SSC) S16.1.0 and S16.0.1 pipelines, respectively. We combined the images produced by the SSC pipeline into mosaics using R. Gutermuth's WCSmosaic IDL package. We then identified all point sources appearing in the resulting mosaics using the IRAF task STARFIND and measured aperture photometry for them using the IRAF task PHOT. The details of these procedures are the same as those described by Luhman et al. (2008). The total exposure times for the IRAC and MIPS images at a given position were 41.6 and ~ 30 s, respectively. The boundaries of the IRAC and MIPS mosaics are indicated in the maps of Chamaeleon I in Figure 1. In a given filter, the three IRAC mosaics cover areas of 0.10, 0.20, and 0.31 deg^2 . The two MIPS mosaics at 24 μm encompass 1.4 and 0.71 deg^2 . The IRAC and MIPS photometric measurements from these images for known members of Chamaeleon I are presented in the Appendix.

Luhman et al. (2008) identified eight promising candidate members of Chamaeleon I in the *Spitzer* images that they analyzed. Those sources exhibit red IRAC and MIPS colors that are indicative of circumstellar disks and are located in the vicinity of known members of the star-forming region. The candidacy of one of these objects, 2MASS J11025374–7722561, is also supported by its optical and near-IR colors (López Martí et al. 2004; Luhman 2007). To assess their membership, we selected for spectroscopy the six candidates that are bright enough for optical spectroscopy, consisting of 2MASS J11020610–7718079, 2MASS J11025374–7722561, Cha J11062854–7618039, 2MASS J11085367–7521359, 2MASS J11100336–7633111 (also known as OTS 32), and 2MASS J11291470–7546256. We also performed spectroscopy on 2MASS J11095493–7635101, which was not discussed by Luhman et al. (2008). It is a promising candidate because of its red *Spitzer* colors and its close proximity to young stars in the Cederblad 112 reflection nebula. Using the new *Spitzer* data from program 30574 that we have reduced in this work, we searched for possible young stars with disks with the same criteria that were employed by Luhman et al. (2008), namely $[3.6] - [4.5] > 0.15$, $[5.8] - [8.0] > 0.3$, and errors less than 0.1 mag in all four bands. From the result-

ing candidates, we selected 2MASS J10533978–7712338 and Cha J11122701–7715173 for spectroscopy. Finally, we included in our spectroscopic sample 2MASS J11091297–7729115, which is the remaining bright candidate member appearing in the optical and near-IR color-magnitude diagrams from Luhman (2007).

3. SPECTROSCOPY OF CANDIDATES

3.1. Observations

We obtained long-slit optical spectra of the 10 candidate members of Chamaeleon I that were selected in § 2 using the Low Dispersion Survey Spectrograph (LDSS-3) on the Magellan II Telescope on the nights of 2007 December 17 and 18. The spectra were taken through a 1.1" slit. The instrument was operated with the VPH All and VPH Red grisms on the first and second nights, respectively, resulting in spectral resolutions of 10 and 5.5 \AA at 7500 \AA . All data were obtained with the slit rotated to the parallactic angle. After bias subtraction and flat-fielding, the spectra were extracted and calibrated in wavelength with arc lamp data. The spectra were then corrected for the sensitivity functions of the detectors, which were measured from observations of a spectrophotometric standard star.

3.2. Spectral Classification

We now examine the LDSS-3 spectra for the evidence of youth that is expected for members of Chamaeleon I. The spectrum of 2MASS J11291470–7546256 exhibits emission lines that are indicative of a galaxy. Although the signal-to-noise ratio of its data is low, we conclude that Cha J11122701–7715173 is probably a background source rather than a low-mass member of the cluster based on the relatively blue slope and absence of late-type spectral features in its spectrum. The remaining eight candidates do show spectral signatures of young objects, such as strong H α emission and weak Na I and K I absorption lines. We also detect He I emission at 6678 \AA from 2MASS J11085367–7521359 and Ca II emission from OTS 32 and Cha J11062854–7618039. Therefore, we classify these eight objects as members of Chamaeleon I. The evidence of youth and membership is compiled in Table 1. When these new members are combined with the membership lists from Luhman (2007) and Luhman et al. (2008), the resulting census of Chamaeleon I contains 237 sources.

To measure spectral types for the eight new members, we have compared their spectra to data for late-type members of Chamaeleon I and other star-forming regions (Luhman 2004, 2007), which were originally classified at optical wavelengths through comparison to averages of dwarfs and giants (Luhman 1999). The resulting classifications are presented in Table 1. The spectra are shown in order of spectral type in Figure 2. The spectral type for Cha J11062854–7618039 is more uncertain than those of the other objects. A reasonable match to its spectrum is produced by both M8 with $A_V \sim 3$ and L0 with $A_V \sim 1$. The latter agrees somewhat better with the data, but a spectrum with a higher signal-to-noise ratio in the TiO band near 7200 \AA is needed for a definitive classification. A spectral type of L0 would make Cha J11062854–7618039 tied with Cha J11070768–7626326 (Luhman et al. 2008) as the coolest

known member of Chamaeleon I.

4. PROPERTIES OF NEW MEMBERS

4.1. Stellar Parameters

To examine the properties of the eight new members of Chamaeleon I, we begin by estimating their extinctions, effective temperatures, bolometric luminosities, and masses. Extinctions were derived from the optical spectra during the process of spectral classification (Luhman 2004, 2007). We have converted our spectral types to effective temperatures with the temperature scale from Luhman et al. (2003). Luminosities have been estimated from J -band photometry in the manner described by Luhman (2007). Because near-IR data are unavailable for Cha J11062854–7618039, we have estimated its J magnitude by combining its $3.6\ \mu\text{m}$ measurement with the average value of $J - [3.6]$ for late-type members of Chamaeleon I that do not have mid-IR excess emission (Luhman et al. 2008). By doing so, we are assuming that the disk emission at $3.6\ \mu\text{m}$ is negligible compared to the stellar photosphere, which is true for most brown dwarfs with disks (Luhman et al. 2005). The uncertainties in A_J , J , BC_J , and the distance modulus ($\sigma \sim 0.13, 0.05, 0.1, 0.13$) correspond to total uncertainties of ± 0.09 in $\log L_{\text{bol}}$. The extinctions, temperatures, and luminosities for the new members of Chamaeleon I are listed in Table 1. We also include the available near-IR photometry for these objects.

The temperatures and luminosities of the new members are plotted on a Hertzsprung-Russell (H-R) diagram in Figure 3. For comparison, we also show the previously known low-mass members of Chamaeleon I (Luhman 2007; Luhman et al. 2008) and the predictions of theoretical evolutionary models (Baraffe et al. 1998; Chabrier et al. 2000). The positions of the three coolest new members in Figure 3 are within the sequence of known members and are indicative of substellar masses. As discussed by Luhman et al. (2008), the precise value of the mass estimate for a young late-type object depends on whether it is derived from the temperature, the luminosity, or both. The five other new members have masses ranging from 0.1 to $0.55 M_{\odot}$ according to the data and models in Figure 3. However, three of these objects, OTS 32, 2MASS J11095493–7635101, and 2MASS J10533978–7712338, appear below the cluster sequence. The resulting isochronal ages ($\tau > 30$ Myr) are unrealistically old considering that these sources exhibit clear signatures of youth ($\tau < 10$ Myr). These anomalously low luminosities may indicate that the stars are seen primarily in scattered light (e.g., edge-on disks) at the shorter wavelengths from which the luminosities were estimated. Indeed, we find that extended emission surrounds 2MASS J11095493–7635101 in the near-IR images of Chamaeleon I obtained by Luhman (2007), supporting this hypothesis. The nature of these sources is investigated further using their spectral energy distributions in § 4.3. We note that OTS 32 was originally identified as a possible member of Chamaeleon I through the detection of K -band excess emission (Oasa et al. 1999; Persi et al. 1999). The faint near-IR magnitudes of this object were suggestive of a substellar mass, but as we have shown, it is probably a low-mass star based on its mid-M spectral type.

4.2. Spatial Distribution

The spatial positions of some of the new members of Chamaeleon I merit discussion. Two of these objects, OTS 32 and 2MASS J11095493–7635101, are within the group of young stars toward the Cederblad 112 reflection nebula, as shown in the optical and IR images in Figure 4. All of the $24\ \mu\text{m}$ sources within that $5' \times 5'$ field are spectroscopically confirmed members of the cluster. Two of the new members, 2MASS J11085367–7521359 and 2MASS J10533978–7712338, are relatively far from the bulk of the stellar population of Chamaeleon I. The former is 1° north of the cloud complex and is separated by $2'$ from the proper motion members RX J1108.8–7519A and RX J1108.8–7519B (Alcalá et al. 1995; Covino et al. 1997; Luhman et al. 2008) and the latter is projected against a small cloudlet on the western edge of Chamaeleon I. Finally, 2MASS J11091297–7729115 is only $4''$ from T39A and T39B. Thus, these stars may comprise a triple system.

4.3. SED Classifications

All but one of the new members of Chamaeleon I were selected for spectroscopy in § 2 based on red mid-IR colors that suggested the presence of circumstellar disks. We now examine the IR spectral energy distributions (SEDs) of these sources in more detail. To construct these SEDs, we use I -band photometry from López Martí et al. (2004), the Third Release of the Deep Near-Infrared Survey of the Southern Sky (DENIS, Epchtein et al. 1999), and the Magellan IMACS images obtained by Luhman (2007), near-IR photometry from 2MASS and Luhman (2007, see Table 1), and mid-IR measurements from IRAC and MIPS that are listed in Table 6 from Luhman et al. (2008) and in the Appendix. The resulting SEDs for the new members are plotted in Figure 5. To determine if long-wavelength excess emission is present, we compare each SED to an estimate of the SED of the stellar photosphere, which is composed of the average colors of diskless stars near the spectral type in question (Luhman et al. 2008). The photospheric SEDs are reddened according to the extinctions in Table 1 and the reddening laws from Rieke & Lebofsky (1985) and Flaherty et al. (2007) and are normalized to the J -band fluxes of the new members, except for 2MASS J11020610–7718079 and Cha J11062854–7618039. Because the available near-IR magnitudes of the former have large uncertainties, the normalization is performed with the average of the J , H , and K_s data. For Cha J11062854–7618039, only IRAC and MIPS measurements are available. Therefore, we scale its photospheric template to the flux at $3.6\ \mu\text{m}$. The emission from brown dwarfs with disks at this wavelength is usually dominated by the photosphere, as discussed in § 4.1 and illustrated in the SEDs for the other late-type objects in Figure 5.

As expected, the seven IR-selected members exhibit significant excess emission at long wavelengths relative to stellar photospheres. The remaining member, 2MASS J11091297–7729115, was identified as a candidate through optical and near-IR color-magnitude diagrams (Luhman 2007). Its SED agrees well with that of a stellar photosphere and shows no evidence of disk emission. To characterize the SEDs quantitatively, we

use spectral slopes defined as $\alpha = d \log(\lambda F_\lambda) / d \log(\lambda)$ (Lada & Wilking 1984; Adams et al. 1987). As in Luhman et al. (2008), we compute slopes between four pairs of bands, 2.2-8, 2.2-24, 3.6-8, and 3.6-24 μm . We deredden these slopes using the extinctions from Table 1 and the reddening law from Flaherty et al. (2007). The resulting values of α_{2-8} , α_{2-24} , $\alpha_{3.6-8}$, and $\alpha_{3.6-24}$ are presented in Table 2. We also include the equivalent widths of the H α emission line measured from our spectra. We classify each object as class I, flat-spectrum, class II, or class III by applying the thresholds from Luhman et al. (2008) to the spectral slopes, which follows the standard classification scheme for SEDs of young stars (Lada 1987; Greene et al. 1994).

The SED classifications produced by α_{2-8} , α_{2-24} , $\alpha_{3.6-8}$, and $\alpha_{3.6-24}$ agree with each other for five sources, but not for OTS 32, 2MASS J11095493–7635101, and 2MASS J10533978–7712338. For the latter three objects, the SEDs become redder with longer wavelengths such that the slopes ending at 8 and 24 μm indicate class II and flat/class I, respectively. The distinctive behavior of these SEDs is indicative of stars that are occulted by circumstellar material, such as edge-on disks (Luhman et al. 2008), which is consistent with the anomalously faint near-IR magnitudes of these objects (§ 4.1). Indeed, the shape of the SED of OTS 32 closely resembles that of 2MASS J04381486+2611399, which is a young brown dwarf in Taurus that has an edge-on disk (Luhman et al. 2007). Thus, we tentatively classify OTS 32 and 2MASS J10533978–7712338 as class II sources with edge-on disks. Because 2MASS J11095493–7635101 exhibits a more steeply rising SED at 24 μm , it could be a class I source. The absence of excess emission at $\lambda < 5 \mu\text{m}$ relative to our estimate for its stellar photosphere may indicate the presence of an inner cavity in its disk and envelope. Our SED classifications for the new members are provided in Table 2. Because the new class I and class II objects were identified as possible members based on evidence of disks, they should not be used in disk fraction measurements for Chamaeleon I unless they are encompassed by the completeness limits of another survey for members that is unbiased in terms of disks.

5. DISCUSSION

⁴ These spectral types were derived in the same manner as the one for the new class I source in Chamaeleon I. Slightly later spectral types for these three Taurus objects were reported by

We conclude with a few remarks concerning notable aspects of the eight new members of Chamaeleon I that we have identified. Three of the new members have spectral types later than M6, and thus are likely to be brown dwarfs. The current census of Chamaeleon I now contains 33 known members later than M6. One of the new late-type members is classified as M8-L0; a type of L0 would make it one of the two coolest known members of the cluster and one of the least massive objects known to harbor a circumstellar disk. Additional optical spectroscopy of this object is needed for a more definitive spectral classification. Seven of our new members were identified as possible members based on red mid-IR colors that indicated the presence of disks. As noted in § 1, a sensitive mid-IR survey of this kind is capable of finding disk-bearing young stars that are heavily obscured. For instance, because stars with edge-on disks are seen primarily in scattered light, they appear sub-luminous in optical color-magnitude diagrams and thus can be overlooked by optical surveys. Indeed, three of the new members exhibit properties that are indicative of edge-on disks. High-resolution images and mid-IR spectroscopy are needed to determine if edge-on disks are present (Luhman et al. 2007). One of the possible edge-on systems has a mass near the hydrogen burning mass limit according to its M5.75 spectral type and could be in the class I stage based on its rising SED from 4.5 to 24 μm . In comparison, the coolest known class I candidates prior to this work were IRAS 04158+2805, IRAS 04248+2612, and IRAS 04489+3042 in Taurus (Kenyon & Hartmann 1995; White & Hillenbrand 2004), which have optical spectral types of M5.25, M4.5, and M4, respectively (Luhman 2006)⁴. Thus, this new object in Chamaeleon I may be one of the least massive known class I sources.

K. L. was supported by grant AST-0544588 from the National Science Foundation. This publication makes use of data products from 2MASS, which is a joint project of the University of Massachusetts and the Infrared Processing and Analysis Center/California Institute of Technology, funded by NASA and the NSF.

White & Hillenbrand (2004).

APPENDIX

SPITZER PHOTOMETRY FOR KNOWN MEMBERS OF CHAMAELEON I

Luhman et al. (2008) presented *Spitzer* photometry for all members of Chamaeleon I that were known at that time and for a sample of candidate members. Those data were measured from all IRAC and MIPS 24 μm images within 3° of the star-forming region, with the exception of program 30574. As described in § 2, we have reduced the data from program 30574 and used them to search for new members. In Table 3, we present our IRAC and MIPS measurements for all known members appearing in those data. Five of the objects that we have confirmed as new members were presented as candidates by Luhman et al. (2008). Thus, their *Spitzer* photometry is provided in that study. One of the new members was identified in the images from program 30574, and therefore is in Table 3. The remaining new members, 2MASS J11091297–7729115 and 2MASS J11095493–7635101, were not in the lists of members and candidates in Luhman et al. (2008). We include all available *Spitzer* measurements for these objects in Table 3. The IRAC data for 2MASS J11091297–7729115 were obtained on 2004 June 10 and the IRAC and MIPS data for 2MASS J11095493–7635101 were obtained on 2004 July 4 and 2004 April 11, respectively. Table 3 and the tables in Luhman et al. (2008) represent a compilation of all IRAC and MIPS 24 μm measurements for all known members of

Chamaeleon I.

We briefly summarize the implications of the new *Spitzer* photometry in Table 3 for our knowledge of the disk population in Chamaeleon I. Combining the data from Luhman et al. (2008) and in Table 3, IRAC and MIPS 24 μ m photometry has been measured for 208 and 166 members, respectively. Only eight of the 237 known members are outside of all of the IRAC and MIPS images of this region. Table 3 provides the first *Spitzer* photometry for eleven previously known members. As a result, the SEDs of these objects were not classified by Luhman et al. (2008). Based on our new photometry, we classify T3A, T4, T5, T7, T8, T16, and T56 as class II and 2MASS J11052272–7709290, Hn 7, Cam 2-42, and CHXR 57 as class III. Luhman et al. (2008) did not compute spectral slopes like the ones in Table 2 for T6, T27, and CHXR 54 because they were outside of the 8 and 24 μ m images considered in that study. As a result, they were classified using the IRAC data that were available at shorter wavelengths. Those classifications are confirmed by the full sets of IRAC and MIPS photometry for these stars that we now have in Table 3. T54 was outside of the IRAC images considered by Luhman et al. (2008), and was classified as class II based on a 24 μ m measurement alone. Our new IRAC data for this star from Table 3 do not exhibit excess emission and instead are consistent with emission from a stellar photosphere. This kind of SED in which excess emission suddenly appears at long IR wavelengths is a signature of a disk with an inner hole, otherwise known as a transitional disk (Calvet et al. 2002, 2005; D’Alessio et al. 2005; Espaillat et al. 2007a,b; Furlan et al. 2007). The presence of a transitional disk has been confirmed through through spectroscopy with the *Spitzer* Infrared Spectrograph (Furlan et al., in preparation). Finally, we find that T14A, ISO 91, T23, T35, and T47 have exhibited significant variability (0.2-0.5 mag) between the IRAC and MIPS images from 2004 that were analyzed by Luhman et al. (2008) and the data from 2007 that are in Table 3. In general, the magnitude change is similar among all of the IRAC bands for a given object and pair of epochs. All of these variable stars are class I or class II, which provides additional evidence that stars with disks exhibit greater mid-IR variability than diskless stars (Liu et al. 1996; Barsony et al. 2005; Luhman et al. 2008).

REFERENCES

- Adams, F. C., Lada, C. J., & Shu, F. H. 1987, *ApJ*, 571, 378
 Alcalá, J. M., Krautter, J., Schmitt, J. H. M. M., Covino, E., Wichmann, R., & Mundt, R. 1995, *A&AS*, 114, 109
 Allen, L. E., et al. 2004, *ApJS*, 154, 363
 Allen, P. R., et al. 2007, *ApJ*, 657, 511
 Allers, K. N., Kessler-Silacci, J. E., Cieza, L. A., & Jaffe, D. T. 2006, *ApJ*, 644, 364
 Allers, K. N., et al. 2007, *ApJ*, 657, 511
 Baraffe, I., Chabrier, G., Allard, F., & Hauschildt, P. H. 1998, *A&A*, 337, 403
 Barsony, M., Ressler, M. E., & Marsh, K. A. 2005, *ApJ*, 630, 381
 Beichman, C. A., Myers, P. C., Emerson, J. P., Harris, S., Mathieu, R., Benson, P. J., & Jennings, R. E. 1986, *ApJ*, 307, 337
 Bertout, C., Robichon, N., & Arenou, F. 1999, *A&A*, 352, 574
 Calvet, N., D’Alessio, P., Hartmann, L., Wilner, D., Walsh, A., & Sitko, M. 2002, *ApJ*, 568, 1008
 Calvet, N., et al. 2005, *ApJ*, 630, L185
 Cambrésy, L., Epchtein, N., Copet, E., de Batz, B., Kimeswenger, S., Le Bertre, T., Rouan, D., & Tiphene, D. 1997, *A&A*, 324, L5
 Chabrier, G., Baraffe, I., Allard, F., & Hauschildt, P. 2000, *ApJ*, 542, L119
 Comerón, F., Neuhauser, R., & Kaas, A. A. 2000, *A&A*, 359, 269
 Comerón, F., Rieke, G. H., Claes, P., Torra, J., & Laureijs, R. J. 1998, *A&A*, 335, 522
 Covino, E., Alcalá, J. M., Allain, S., Bouvier, J., Terranegra, L., & Krautter, J. 1997, *A&A*, 328, 187
 D’Alessio, P., et al. 2005, *ApJ*, 621, 461
 Epchtein, N., et al. 1999, *A&A*, 349, 236
 Espaillat, C., et al. 2007a, *ApJ*, 664, L111
 Espaillat, C., et al. 2007b, *ApJ*, 670, L135
 Fazio, G. G., et al. 2004, *ApJS*, 154, 10
 Flaherty, K. M., Pipher, J. L., Megeath, S. T., Winston, E. M., Gutermuth, R. A., Muzerolle, J., Allen, L. E., & Fazio, G. G. 2007, *ApJ*, 663, 1069
 Furlan, E., et al. 2007, *ApJ*, 644, 1176
 Greene, T. P., Wilking, B. A., André, P., Young, E. T., & Lada, C. J. 1994, *ApJ*, 434, 614
 Gutermuth, R. A., Megeath, S. T., Muzerolle, J., Allen, L. E., Pipher, J. L., Myers, P. C., & Fazio, G. G. 2004, *ApJS*, 154, 374
 Haisch, K. E., Lada, E. A., & Lada, C. J. 2001, *ApJ*, 553, L153
 Kenyon, S. J., & Hartmann, L. 1995, *ApJS*, 101, 117
 Kenyon, S. J., Hartmann, L. W., Strom, K. M., & Strom, S. E. 1990, *AJ*, 99, 869
 Lada, C. J. 1987, in *IAU Symp. 115, Star Forming Regions*, ed. M. Peimbert & J. Jugaku (Dordrecht: Reidel), 1
 Lada, C. J., Muench, A. A., Haisch, K. E., Lada, E. A., Alves, J. F., Tollestrup, E. V., & Willner, S. P. 2000, *ApJ*, 120, 3162
 Lada, C. J., & Wilking, B. A. 1984, *ApJ*, 287, 610
 Liu, M. C., et al. 1996, *ApJ*, 461, 334
 López Martí, B., Eisloffel, J., Scholz, A., & Mundt, R. 2004, *A&A*, 416, 555
 Luhman, K. L. 1999, *ApJ*, 525, 466
 Luhman, K. L. 2004, *ApJ*, 602, 816
 Luhman, K. L. 2006, *ApJ*, 645, 676
 Luhman, K. L. 2007, *ApJS*, 173, 104
 Luhman, K. L., Adame, L., D’Alessio, P., Calvet, N., Hartmann, L., Megeath, S. T., & Fazio, G. G. 2005, *ApJ*, 635, L93
 Luhman, K. L., Stauffer, J. R., Muench, A. A., Rieke, G. H., Lada, E. A., Bouvier, J., & Lada, C. J. 2003, *ApJ*, 593, 1093
 Luhman, K. L., Whitney, B. A., Meade, M. R., Babler, B. L., Indebetouw, R., Bracker, S., & Churchwell, E. B. 2006, *ApJ*, 647, 1180
 Luhman, K. L., et al. 2007, *ApJ*, 666, 1219
 Luhman, K. L., et al. 2008, *ApJ*, 675, 1375
 Megeath, S. T., et al. 2004, *ApJS*, 154, 367
 Muench, A. A., Lada, C. J., Luhman, K. L., Muzerolle, J., & Young, E. 2007, *AJ*, 134, 411
 Muzerolle, J., et al. 2004, *ApJS*, 154, 379
 Natta, A., & Testi, L. 2001, *A&A*, 376, L22
 Oasa, Y., Tamura, M., & Sugitani, K. 1999, *ApJ*, 526, 336
 Pascucci, I., Apai, D., Henning, Th., & Dullemond, C. P. 2003, *ApJ*, 590, L111
 Persi, P., Marenzi, A. R., Kaas, A. A., Olofsson, G., Nordh, L., & Roth, M. 1999, *AJ*, 117, 439
 Persi, P., et al. 2000, *A&A*, 357, 219
 Rieke, G. H., & Lebofsky, M. J. 1985, *ApJ*, 288, 618
 Rieke, G. H. et al. 2004, *ApJS*, 154, 25
 Skrutskie, M., et al. 2006, *AJ*, 131, 1163
 Werner, M. W., et al. 2004, *ApJS*, 154, 1
 White, R. J., & Hillenbrand, L. A. 2004, *ApJ*, 616, 998
 Whittet, D. C. B., Prusti, T., Franco, G. A. P., Gerakines, P. A., Kilkenny, D., Larson, K. A., & Wesselius, P. R. 1997, *A&A*, 327, 1194
 Wichmann, R., Bastian, U., Krautter, J., Jankovics, I., & Ruciński, S. M. 1998, *MNRAS*, 301, L39

TABLE 1
 NEW MEMBERS OF CHAMAELEON I

Name	Spectral Type ^a	$T_{\text{eff}}^{\text{b}}$ (K)	A_J	L_{bol} (L_{\odot})	Membership Evidence ^c	J^{d}	H^{d}	K_s^{d}
2M J10533978–7712338	M2.75	3451	0.63	0.032 ^e	ex, A_V	13.28±0.02	12.14±0.03	11.58±0.02
2M J11020610–7718079	M8	2710	0.56	0.0031	e,ex,NaK	15.63±0.08	14.81±0.07	14.26±0.09
2M J11025374–7722561 ^f	M8.5	2555	0.21	0.0015	ex,NaK	16.05±0.11	...	14.70±0.13
Cha J11062854–7618039	M8-L0	~2400	~0.3	~0.001	e,ex,NaK
2M J11085367–7521359 ^g	M1.5	3632	0.28	0.23	e,ex	10.98±0.03	10.07±0.03	9.56±0.03
2M J11091297–7729115 ^h	M3	3415	0.14	0.16	NaK	11.00±0.04	10.27±0.03	9.98±0.03
2M J11095493–7635101	M5.75	3024	0.42	0.0014 ^e	e,ex,NaK, A_V	16.34±0.03	15.47±0.02	15.13±0.03
2M J11100336–7633111 ⁱ	M4±1	3270	1.7	0.0025 ^e	e,ex, A_V	17.06±0.02	15.29±0.02	14.01±0.02

^a Uncertainties are ± 0.25 subclass unless noted otherwise. These uncertainties represent the precision within the optical classification scheme adopted in this work (Luhman 1999).

^b Converted from the spectral types using the temperature scale from Luhman et al. (2003). In addition to the errors in the spectral type, these temperature estimates are subject to a systematic uncertainty in the temperature scale (Luhman et al. 2008), which is probably at least ± 100 K.

^c Membership in Chamaeleon is indicated by $A_V \gtrsim 1$ and a position above the main sequence for the distance of Chamaeleon (“ A_V ”), strong emission lines (“e”), Na I and K I strengths intermediate between those of dwarfs and giants (“NaK”), or IR excess emission (“ex”).

^d From the ISPI images of Luhman (2007) for 2M J11095493–7635101 and 2M J11100336–7633111 and from the Point Source Catalog of the Two-Micron All-Sky Survey (2MASS, Skrutskie et al. 2006) for the remaining sources.

^e This star may have an edge-on disk. If so, this luminosity estimate is not reliable.

^f [LES2004] 424.

^g 2' from RX J1108.8–7519A and RX J1108.8–7519B.

^h 4'' from T39A and T39B.

ⁱ OTS 32. 18'' from Hn 11.

 TABLE 2
 H α AND SPECTRAL SLOPES FOR NEW MEMBERS OF CHAMAELEON I

Name	$W_{\lambda}(\text{H}\alpha)$ (\AA)	$\alpha(2-8 \mu\text{m})$	$\alpha(2-24 \mu\text{m})$	$\alpha(3.6-8 \mu\text{m})$	$\alpha(3.6-24 \mu\text{m})$	SED Class
2M J10533978–7712338	8±1	–1.58	–0.50	–0.90	0.06	II
2M J11020610–7718079	~100	–1.49	–1.09	–1.64	–1.04	II
2M J11025374–7722561	~10	–1.65	–1.01	–1.87	–0.94	II
Cha J11062854–7618039	>100	–1.67	–1.04	II
2M J11085367–7521359	82±3	–1.68	–1.14	–2.01	–1.14	II
2M J11091297–7729115	6.3±0.3	–2.77	...	–3.00	...	III
2M J11095493–7635101	40±10	–0.31	0.88	1.06	1.76	I or II
2M J11100336–7633111	~20	–0.64	0.36	–0.61	0.62	II

TABLE 3
Spitzer PHOTOMETRY FOR KNOWN MEMBERS OF CHAMAELEON I

2MASS ^a	Name	[3.6]	[4.5]	[5.8]	[8.0]	[24]
J10533978–7712338	...	11.49±0.02	11.09±0.02	10.60±0.03	9.76±0.04	5.28±0.04
J10555973–7724399	T3A	out	out	out	out	2.37±0.04
J10563044–7711393	T4	8.31±0.02	out	7.58±0.03	out	3.25±0.04
J10574219–7659356	T5	8.74±0.02	out	8.07±0.03	out	4.35±0.04
J10580597–7711501	...	out	out	out	out	7.21±0.05
J10581677–7717170	T6	out	out	out	out	1.94±0.04
J10590108–7722407	T7	out	out	out	out	3.45±0.04
J10590699–7701404	T8	out	out	out	out	1.78±0.04
J11013205–7718249	ESO H α 554	13.08±0.02	out	12.92±0.04	out	...
J11020610–7718079	...	13.43±0.02	out	12.81±0.04	out	9.49±0.22
J11025374–7722561	[LES2004] 424	out	out	out	out	9.65±0.18
J11025504–7721508	T12	out	out	out	out	5.88±0.04
J11034764–7719563	Hn 2	9.70±0.02	out	9.53±0.03	out	9.41±0.18
J11035682–7721329	CHXR 12	out	out	out	out	9.31±0.15
J11042275–7718080	T14A	10.59±0.02	9.79±0.02	8.95±0.03	7.71±0.04	3.40±0.04
J11044258–7741571	ISO 52	out	9.81±0.02	out	9.01±0.04	out
J11045701–7715569	T16	9.80±0.02	9.57±0.02	9.18±0.04	8.63±0.04	6.11±0.04
J11051467–7711290	Hn 4	9.26±0.02	9.16±0.02	9.12±0.03	9.18±0.04	8.92±0.11
J11052272–7709290	...	11.48±0.02	11.39±0.02	11.38±0.03	11.37±0.04	...
J11054300–7726517	CHXR 15	out	out	out	out	9.09±0.14
J11061540–7721567	Ced 110-IRS2/T21	6.25±0.02	out	6.14±0.03	out	5.58±0.07
J11062942–7724586	...	out	out	out	out	8.70±0.20
...	Cha-MMS1	8.94±0.15
J11063799–7743090	Cha H α 12	out	11.21±0.02	out	11.14±0.03	out
J11064346–7726343	T22	out	out	out	out	8.86±0.17
J11064510–7727023	CHXR 20	out	out	out	out	4.41±0.04
J11064658–7722325	Ced 110-IRS4	10.91±0.05	out	9.23±0.04	out	2.02±0.04
J11065803–7722488	ISO 86	10.22±0.02	out	8.27±0.03	out	3.66±0.04
J11065906–7718535	T23	9.76±0.02	9.41±0.02	8.96±0.03	7.99±0.04	5.07±0.04
J11070369–7724307	...	out	out	out	out	7.30±0.05
J11070919–7723049	Ced 110-IRS6	8.00±0.02	out	6.39±0.03	out	1.64±0.04
J11070925–7718471	ISO 91	10.56±0.02	10.15±0.02	9.76±0.03	8.98±0.04	5.35±0.04
J11071148–7746394	CHXR 21	out	9.25±0.02	out	9.24±0.04	out
J11071622–7723068	ISO 97	9.42±0.02	out	8.24±0.03	out	4.00±0.04
J11072142–7722117	B35	9.55±0.02	out	8.30±0.03	out	3.55±0.04
J11072825–7652118	T27	9.06±0.02	8.74±0.02	8.47±0.03	7.63±0.04	4.53±0.04
J11073832–7747168	ESO H α 560	10.66±0.02	out	10.56±0.03	out	out
J11075588–7727257	CHXR 28	out	out	out	out	7.29±0.04
J11075730–7717262	CHXR 30B	8.16±0.02	7.56±0.02	7.21±0.03	6.82±0.04	3.95±0.04
J11075993–7715317	ESO H α 561	10.73±0.02	10.57±0.02	10.54±0.03	10.55±0.03	...
J11080002–7717304	CHXR 30A	8.49±0.02	8.28±0.02	7.97±0.03	7.32±0.03	5.44±0.11
J11082570–7716396	...	13.56±0.02	13.08±0.02	12.73±0.04	12.14±0.04	9.44±0.18
J11082650–7715550	ISO 147	11.58±0.02	11.22±0.02	10.91±0.03	10.27±0.03	7.63±0.05
J11083905–7716042	T35	8.71±0.02	8.45±0.02	8.27±0.03	8.21±0.04	4.75±0.04
J11085464–7702129	T38	8.58±0.02	8.09±0.02	7.73±0.03	7.20±0.03	3.96±0.04
J11090512–7709580	Hn 7	10.67±0.02	10.55±0.02	10.61±0.03	10.57±0.03	...
J11091297–7729115	...	9.80±0.08	9.77±0.08	9.64±0.10	9.91±0.12	...
J11092913–7659180	[LES2004] 602	11.75±0.02	11.62±0.02	11.56±0.03	11.53±0.04	...
J11093777–7710410	Cam 2-42	8.69±0.02	8.55±0.02	8.41±0.03	8.43±0.03	7.94±0.07
J11094260–7725578	C7-1	out	out	out	out	6.55±0.04
J11094742–7726290	B43	out	out	out	out	4.41±0.04
J11094866–7714383	ISO 209	11.28±0.02	10.82±0.02	10.46±0.03	9.85±0.03	7.25±0.04
J11095336–7728365	ISO 220	out	out	out	out	7.25±0.05
J11095493–7635101	...	15.00±0.13	14.43±0.23	...	11.59±0.08	5.30±0.20
J11100785–7727480	ISO 235	out	out	out	out	6.36±0.04
J11102852–7716596	Hn 12W	10.37±0.02	10.25±0.02	10.26±0.03	10.22±0.04	...
J11103481–7722053	[LES2004] 405	9.65±0.02	9.52±0.02	9.42±0.03	9.48±0.03	9.06±0.11
J11103644–7722131	ISO 250	10.15±0.02	10.07±0.02	9.98±0.03	9.94±0.04	9.61±0.12
J11104141–7720480	ISO 252	11.45±0.02	11.02±0.02	10.59±0.03	9.75±0.03	7.00±0.04
J11104959–7717517	T47	8.92±0.02	8.35±0.02	7.76±0.03	6.63±0.04	3.00±0.04
J11105076–7718031	ESO H α 568	10.38±0.02	10.28±0.02	10.22±0.03	10.17±0.03	...
J11105359–7725004	ISO 256	9.67±0.02	out	8.70±0.03	out	4.90±0.04
J11105597–7645325	Hn 13	out	9.10±0.02	out	8.02±0.03	out
J11112260–7705538	ISO 274	10.43±0.02	10.35±0.02	10.29±0.03	10.30±0.03	...
J11120288–7722483	...	12.10±0.02	12.00±0.02	11.92±0.03	11.94±0.04	...
J11120351–7726009	ISO 282	10.83±0.02	out	10.13±0.03	out	6.87±0.05
J11122250–7714512	...	13.89±0.02	out	13.55±0.05	out	...
J11123099–7653342	[LES2004] 601	12.59±0.02	12.47±0.02	12.39±0.04	12.36±0.05	...
J11124210–7658400	CHXR 54	9.41±0.02	9.43±0.02	9.35±0.03	9.36±0.03	9.35±0.11
J11124268–7722230	T54	7.81±0.02	7.83±0.02	7.75±0.03	7.66±0.03	4.85±0.04
J11124861–7647066	Hn 17	out	out	out	out	7.01±0.04
J11132012–7701044	CHXR 57	9.79±0.02	out	9.74±0.03	out	9.33±0.15
J11173700–7704381	T56	out	out	out	out	4.22±0.04

NOTE. — Entries of “...” and “out” indicate measurements that are absent because of non-detection and a position outside the field of view of the filter for the observations in program 30574, respectively, except for 2MASS J11091297–7729115. For this star, the non-detection at 24 μ m refers to images from program 37 obtained on 2005 February 27.

^a 2MASS Point Source Catalog.

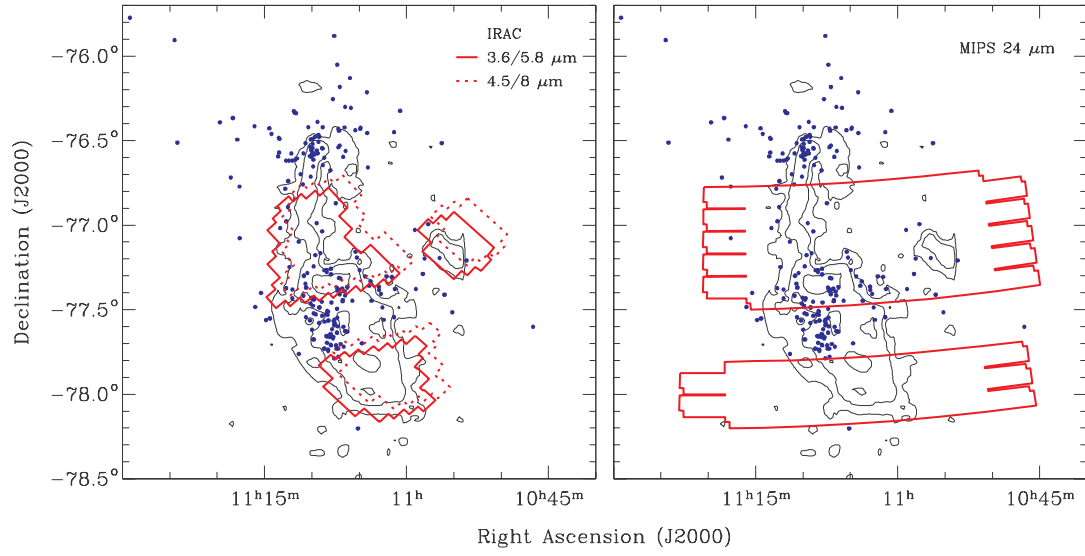


FIG. 1.— Fields in the Chamaeleon I star-forming region that have been imaged with IRAC (*left*) and MIPS (*right*) in *Spitzer* program 30574. The known members of the cluster are indicated (*points*). The contours represent the extinction map of Cambr esy et al. (1997) at intervals of $A_J = 0.5, 1,$ and 2 .

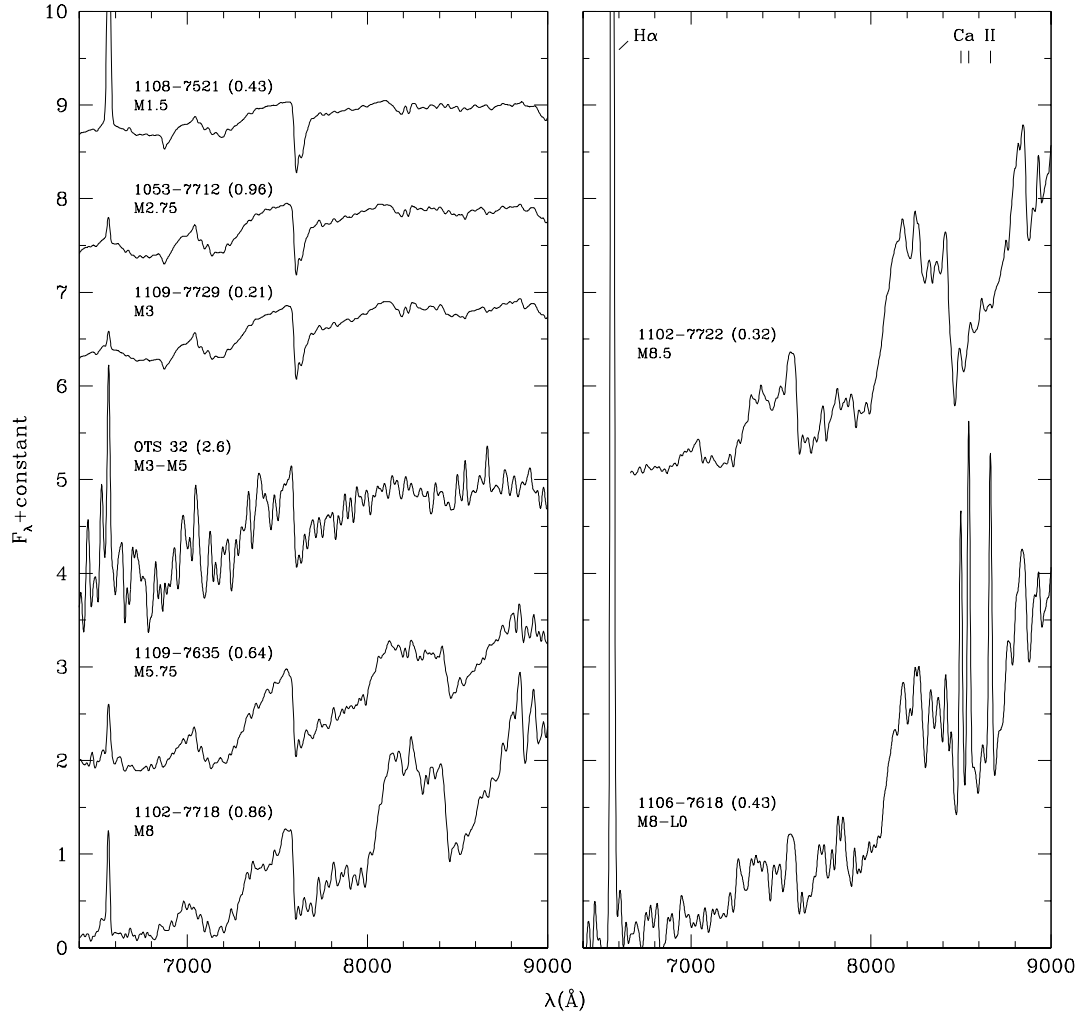


FIG. 2.— Optical spectra of new members of Chamaeleon I. The spectra have been corrected for extinction, which is quantified in parentheses by the magnitude difference of the reddening between 0.6 and 0.9 μm ($E(0.6 - 0.9)$). The data are displayed at a resolution of 18 \AA and are normalized at 7500 \AA .

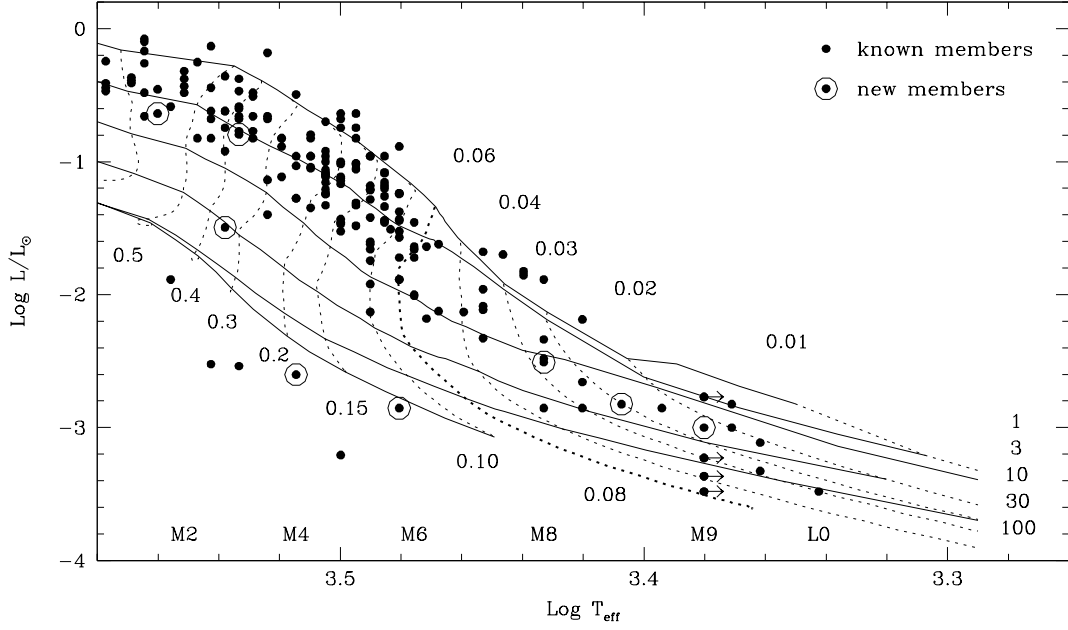


FIG. 3.— H-R diagram for all known low-mass stars and brown dwarfs in Chamaeleon I (Luhman 2007; Luhman et al. 2008, *points*). The sources classified as new members through spectroscopy in Figure 2 are indicated (*circled points*). These data are shown with the theoretical evolutionary models of Baraffe et al. (1998) ($0.1 < M/M_{\odot} \leq 1$) and Chabrier et al. (2000) ($M/M_{\odot} \leq 0.1$), where the mass tracks (*dotted lines*) and isochrones (*solid lines*) are labeled in units of M_{\odot} and Myr, respectively.

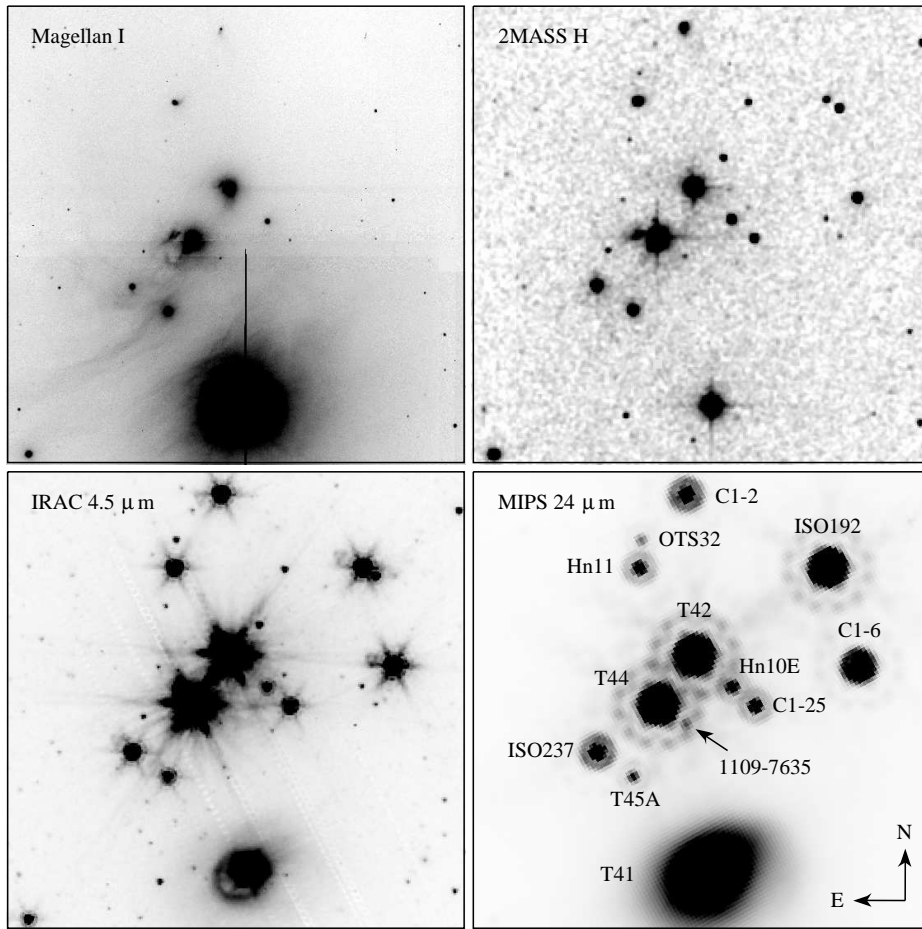


FIG. 4.— Optical and IR images of the region surrounding the Cederblad 112 reflection nebula in Chamaeleon I ($5' \times 5'$). All known members of the star-forming region within this area are labeled. OTS 32 and 2MASS J11095493–7635101 have been classified as new members through the spectra in Figure 2.

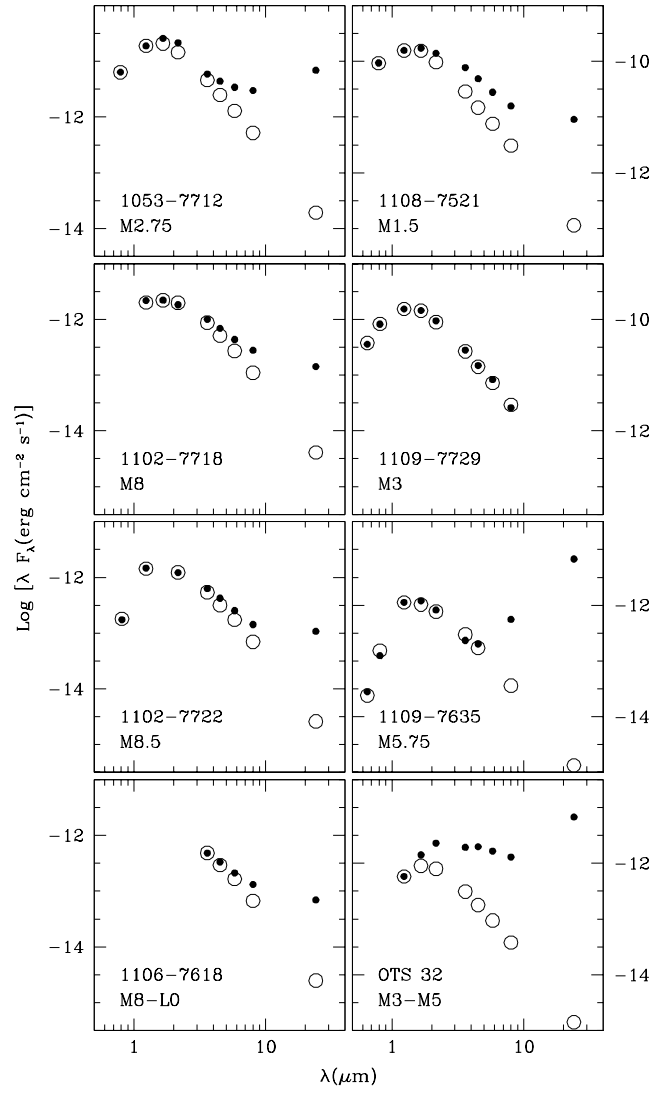


FIG. 5.— SEDs for new members of Chamaeleon I (*points*). Each object is compared to the SED of a stellar photosphere at the same spectral type (*circled points*). The photospheric SEDs have been reddened according to the extinction estimates in Table 1 and have been scaled to the J -band fluxes of the new members, except for 2MASS J11020610–7718079 and Cha J11062854–7618039, for which the photospheres are scaled to JHK_s and $3.6 \mu\text{m}$, respectively.